

Dislocation nucleation from a sharp corner in silicon

Satoshi Izumi^{1,2,a)} and Sidney Yip²

¹*Department of Mechanical Engineering, School of Engineering, The University of Tokyo, Bunkyo-ku, Tokyo 1138656, Japan*

²*Department of Nuclear Science and Engineering and Department of Materials Science and Engineering, Massachusetts Institute of Technology, Cambridge, Massachusetts 02139, USA*

(Received 28 March 2008; accepted 29 May 2008; published online 4 August 2008)

By combining molecular dynamics simulation with reaction pathway sampling, we have observed the nucleation of a three-dimensional dislocation loop from a sharp corner in silicon and investigated the shear stress dependence of the activation energy and saddle-point configuration. The nucleated shuffle-set half-loop consisted of two 60° segments and one screw segment, each lying along a Peierls valley. The half-hexagonal shape is in good agreement with experiments at low temperature. Under high stress (90%–95% of athermal shear stress), the dislocation embryo is far from perfect, with half-size Burgers vector (about 0.2 nm) and a 0.4–0.7 nm radius forming a diffuse core region. A consequence is that the Rice–Thompson theory gives incorrect predictions regarding the activation energy and saddle-point configuration. With decreasing applied stress (less than 70%), the embryo approaches that of a perfect dislocation. © 2008 American Institute of Physics.

[DOI: 10.1063/1.2963487]

I. INTRODUCTION

The stress-induced dislocation loop in silicon devices leads to charge leakage and electrical shorting between devices.^{1,2} Because it can seriously degrade the performance of devices, many researchers have been working on the problem from experimental^{3,4} and theoretical approaches^{5–7} for the past 30 years. Recently, Schwarz *et al.* analyzed the dislocation dynamics in actual devices using his original code⁸ and succeeded in reproducing its configurations.^{9,10} However, since the event of dislocation nucleation, which occurs at an atomic level, is beyond the scale of dislocation theory, they needed to put an initial dislocation loop with 1–5 nm radii at a stress concentration point to mimic the nucleation process. Schwarz also tried to find the critical loop size under various stress fields and concluded that atomistic modeling is required to treat this problem in a serious manner.¹¹

Even though there have been many contributions to dislocation mobility in silicon from an atomistic landscape,^{12,13} little is known about the dislocation nucleation. Godet *et al.* have performed simulations of dislocation nucleation from a surface step in silicon using empirical potential¹⁴ and first-principles calculation.¹⁵ They observed the nucleation of a shuffle-set dislocation loop and obtained the critical conditions. However, since they employed a thin two-dimensional-like model, a straight dislocation was emitted from a surface step. Therefore, they did not discuss the activation barrier and saddle-point configuration of the dislocation embryo.

Generally, dislocation nucleation can occur when the system overcomes an activation energy barrier via thermal fluctuation. Therefore, such a perspective is indispensable to discuss the nucleation process at finite temperature. Recently, Zhu *et al.*^{16,17} have conducted an atomistic simulation of the saddle-point configuration and activation energy for the

nucleation of a three-dimensional (3D) dislocation loop from a stressed crack tip in single crystal Cu. They employed a 3D model that can deal with the dislocation loop nucleation and succeeded in obtaining an activation energy and critical loop configuration by using the nudged elastic-band (NEB) method.

We applied their framework to the dislocation nucleation in covalent-bond silicon. Our employed system is a sharp corner, which is well known as one of the popular dislocation sources in semiconductor devices.^{1–11} Our final goal is to provide a dislocation dynamics simulation with a critical condition for dislocation nucleation. Such a smooth connection would allow for more accurate prediction of the dislocation behaviors in semiconductor silicon. It should be noted that we focus on the ductile fracture (dislocation nucleation) of silicon, while Zhu *et al.*¹⁸ focused on brittle fracture (crack extension).

II. MOLECULAR DYNAMICS SYSTEM

As a first step, molecular dynamics (MD) simulations were conducted to observe the critical athermal strain (γ_{ath}). The simulation model is shown in Fig. 1. A rectangular hole whose x and z sizes were 1/4 of the cell size was created in the model so as to make a sharp corner. Periodic boundary conditions were imposed in all directions. The system size was $23.0 \times 11.5 \times 22.8 \text{ nm}^3$ and included 289 800 atoms. Constant low-temperature (1 K) simulations were carried out in order to reduce the thermal fluctuation. The Stillinger–Weber (SW) potential¹⁹ was employed, along with the Verlet method with a 1 fs time step. In order to avoid phase-transformation problems,²⁰ pure shear stress was applied to a (111)[01 $\bar{1}$] slip system. Namely, the shape of the MD cell was changed so that the resolved shear stress of the (111)

^{a)}Electronic mail: izumi@fml.t.u-tokyo.ac.jp.

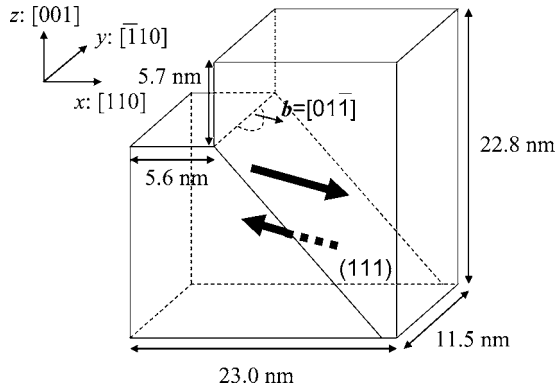


FIG. 1. Simulation model for MD. Resolved shear stress is applied to a $(111)[01\bar{1}]$ slip system.

$\times[01\bar{1}]$ slip system was maximized. As a result, a dislocation loop is subject to the shear stress shown as the arrow in Fig. 1.

When the applied resolved shear strain reached 5.1% (averaged resolved shear stress was 3.5 GPa), a shuffle-set dislocation loop involving two 60° segments and one screw segment was nucleated from a sharp corner. No phase transition to the amorphous phase or twin phase was present. In Fig. 2, snapshots are shown by using the slip-vector representation,²¹ which is a measure of how far an atom has moved relative to its nearest-neighbor and is similar in definition to the Burgers vector. The red atoms show the complete slipped area, and the blue atoms show the small-slipped area. The outline of the colored region indicates the dislocation core region or surface region. In an initial stage, the dislocation embryo is nucleated. It then grows and becomes a perfect dislocation loop whose maximum slip vector reaches that of the Burgers vector. Unlike the nucleated dislocation loop in Cu,¹⁶ the dislocation elongates along different Peierls valleys and shows a half-hexagonal shape. Historically, it is well known that the dislocation loop in silicon has a hexagonal shape whose edges are parallel to the $\langle 110 \rangle$

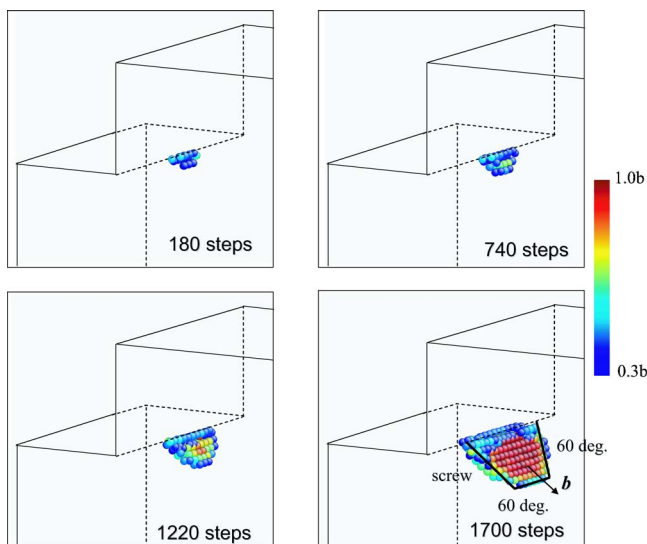


FIG. 2. (Color online) Snapshots of a dislocation nucleation from a sharp corner in silicon.

Peierls valley on the $\{111\}$ slip plane.^{22,23} In recent low-temperature experiments, such hexagonal loops were also observed.²⁴ It can be said that our simulation is in good agreement with the experimental results.

At high temperature, it is widely accepted that glide-set dislocation can move more easily than shuffle-set dislocation based on experimental^{25,26} and theoretical approaches.^{27,28} However, it is also known that shuffle-set perfect dislocation has a lower unstable stacking fault energy (γ_{us}), which is considered to be closely related to dislocation nucleation²⁹ than glide-set partial dislocation. This result was confirmed by the system employing the SW potential (shuffle set, 0.83 J/m^2 ; glide set, 3.08 J/m^2)³⁰ and that employing the density functional theory (DFT) scheme (shuffle set, 1.67 J/m^2 ; glide set, 1.91 J/m^2).³¹ A series of recent experiments³²⁻³⁴ suggests that shuffle-set dislocations are nucleated at low temperature (as low as 77 K). We believe that shuffle-set dislocation could be nucleated under high stress in the semiconductor devices. However, such so-called shuffle-glide controversy has not yet been resolved and is still going on.

It is noted that the shear stress in this system is not homogeneous but is inhomogeneous around the sharp corner. In the vicinity of the sharp corner, the shear stress distribution becomes $\tau = Kr^{-0.2}$. Here, r is the distance from the corner and K is a prefactor. This stress distribution was confirmed by the finite element method simulation employing the same geometrical system.³⁵ The maximum atomistic shear stress reaches approximately 6–7 GPa at a point located 1 nm apart from the corner.

III. REACTION PATHWAY

In order to obtain activation barriers and saddle-point configurations under various stress levels, we apply the NEB method.³⁶⁻³⁸ We have incorporated various techniques such as the improved tangent method,³⁶ climbing method,³⁷ and free-end method.³⁸ Since the setup of initial images greatly affects the convergence of NEB calculation, we carefully pick up 20 atomic configurations from snapshots of MD as initial NEB images. The calculation is considered to be converged when the potential force on each replica vertical to the path becomes less than 0.005 eV/\AA . Our approach is similar to that of Zhu¹⁶ and Boyer.³⁹

Dependence of the activation energy on the shear strain normalized by the athermal strain is shown in Fig. 3 (left). The curve can be fitted by $\Delta E = A(1 - \gamma/\gamma_{ath})^n$. Here, $A = 111.5 \text{ eV}$, $n = 1.87$, and $\gamma_{ath} = 0.051$ are obtained. The exponent n is similar to the case of homogeneous nucleation ($A = 13.7$ and $n = 1.82$),³⁹ nucleation from vacancy ($A = 14.3$ and $n = 1.94$),³⁹ and nucleation from a sharp corner ($A = 7.4$ and $n = 1.75$)⁴⁰ in copper (Mishin potential⁴¹). A prefactor A is approximately 6–15 times larger than that of copper. The prefactor would reflect a higher Peierls barrier of covalent-bonding crystal. The unstable stacking fault energies (γ_{us}) of silicon and copper obtained by using respective interatomic potentials (SW potential and Mishin potential) are 0.83 J m^{-2} and 0.16 J m^{-2} , respectively. There might be any relationship between ΔE and γ_{us} .

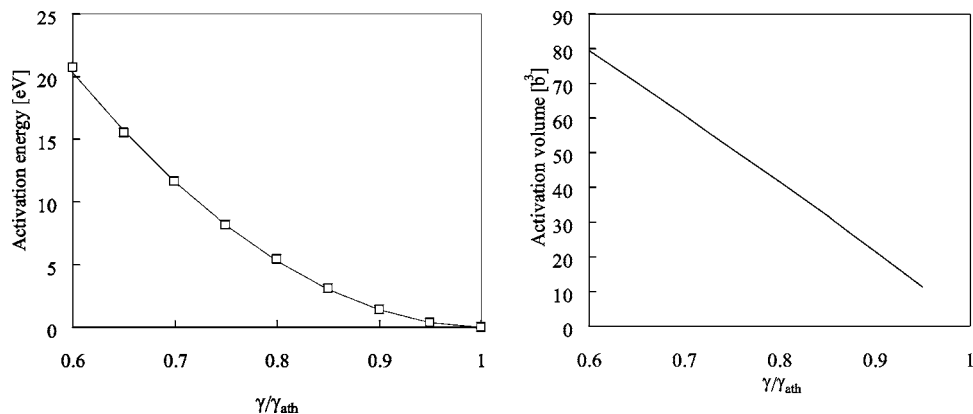


FIG. 3. Dependence of activation energy (left) and activation volume (right) on shear strain for the dislocation nucleation from a sharp corner in silicon.

It should be noted that our comparison study is very limited. For general discussion about physical meaning of A and n , the dependences of A and n on the stress field and material need to be investigated further.

The activation volume defined by the first-order differential of the activation energy with respect to shear stress is also shown in Fig. 3 (right). The activation volume is also larger than that in copper.

It should be noted that Pizzagalli *et al.*⁴² showed that the core properties of screw dislocation in silicon depend on the MD potential used. In order to obtain quantitative result, our results should be also verified by more-sophisticated method such as DFT and tight-binding MD.

In Fig. 4, the saddle-point configurations of a dislocation

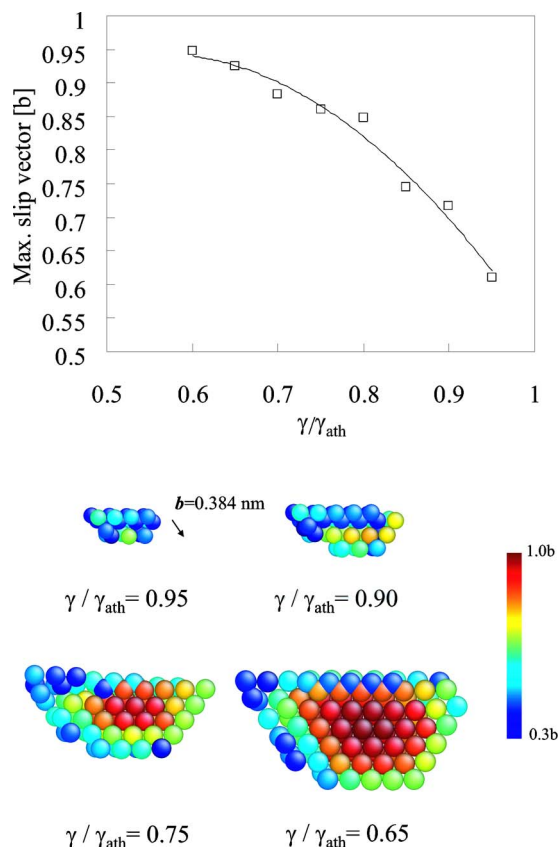


FIG. 4. (Color online) (Top) Maximum inelastic displacement of the saddle-point configuration. (Bottom) Various saddle-point configurations of the loop nucleation from a sharp corner (dislocation embryo).

embryo whose color shows the absolute value of slip vector (bottom) and the dependence of the maximum inelastic displacement of the dislocation embryo on shear strain (top) are shown. In the case of $\gamma/\gamma_{\text{ath}}=0.90\text{--}0.95$, the inelastic displacement of the dislocation embryo, which is defined by the length of the slip vector, is approximately 60%–70% of the length of the Burgers vector. Its direction almost coincides with that of the original perfect dislocation. The radius is 0.4–0.7 nm. Since the dislocation loop is so small, almost the entire loop region is regarded as a diffuse core region. That dislocation loop would be beyond the scale of the dislocation theory. Therefore, direct transfer of the dislocation configuration to the dislocation dynamics might be meaningless and impossible. However, our scheme could provide a dislocation dynamics simulation with a criterion concerning dislocation nucleation.

As the applied stress decreases ($\gamma/\gamma_{\text{ath}}=0.70$), the maximum inelastic displacement approaches that of the Burgers vector and the dislocation embryo approaches that of perfect dislocation. In this scale, the dislocation theory would be effective. However, the activation energy (>10 eV) becomes so high that the system cannot overcome it.

Finally, in order to make clarify the size effect, we conducted the same simulation with a smaller model whose cell sizes are 1/3 those of the original one. This model proved that an activation energy above $\gamma/\gamma_{\text{ath}}=0.85$ (saddle-point loop radius is approximately 15 nm) is not affected by the cell-size effect. It indicated that if the loop radius exceeds 45 nm in the larger model, the result would be subject to a cell-size effect. However, all the resulting radii are below 25 nm. Therefore, we believe that the size effect should not affect the accuracy of the activation energy and the saddle-point configuration reported here.

IV. COMPARISON WITH THE RICE–THOMPSON THEORY

Classical Rice–Thompson (RT) theory⁴³ has been used as a simple way to estimate the critical condition for dislocation nucleation.⁴⁴ Here, we investigate the difference between our atomistic approach and the classical approach. As we indicated, the shear stress in the vicinity of a sharp corner shows $\tau=Kr^{-0.2}$. Using this distribution, the critical condition for dislocation nucleation can be estimated as $K_{\text{crit}}=0.050$ GPa $\text{m}^{0.2}$ for the RT model and 0.106 for our model. It

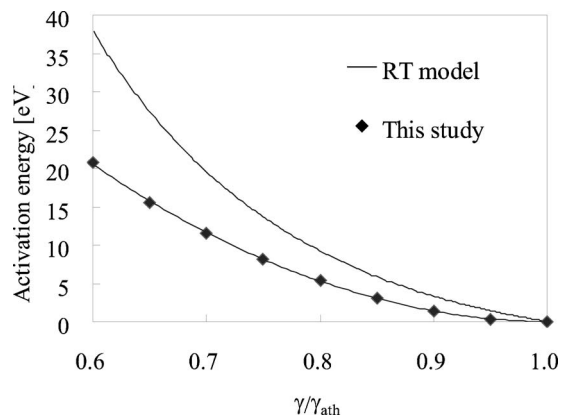


FIG. 5. Comparison of the activation energy curve with the RT model.

should be noted that the RT model underestimates the athermal strain (stress) by half. The dependence of the activation energy on shear strain is shown in Fig. 5. It is found that the RT model overestimates the activation energy by a factor of approximately 2. Rice²⁹ has also proposed a more-sophisticated concept for the dislocation nucleation. It is worth comparing this concept to our new scheme.

V. CONCLUSION

In conclusion, the combination of the MD simulation with reaction pathway sampling enables us to evaluate the critical condition of the dislocation nucleation process. The dislocation theory is inaccessible to such a nucleation process due to its size limitation, and only an atomistic approach can solve that problem. We believe our scheme provides insight into the dislocation nucleation phenomena in semiconductor devices.

ACKNOWLEDGMENTS

S.I. acknowledges R. D. Boyer, X. Lin, and J. Li for their kind discussions.

¹P. M. Fahey, S. R. Mader, S. R. Stiffler, R. L. Mohler, J. D. Mis, and J. A. Slinkman, *IBM J. Res. Dev.* **36**, 158 (1992).

²S. M. Hu, *J. Appl. Phys.* **70**, R53 (1991).

³S. Isomae, *J. Appl. Phys.* **57**, 216 (1985).

⁴H. Ohta, H. Miura, and M. Kitano, *Mater. Sci. Res. Int.* **4**, 261 (1998).

⁵J. Vanhellefont, S. Amelinckx, and C. Claeys, *J. Appl. Phys.* **61**, 2170 (1987).

⁶S. Isomae, *J. Appl. Phys.* **52**, 2782 (1981).

⁷Z. Zhang, J. Yoon, and Z. Suo, *Appl. Phys. Lett.* **89**, 261912 (2006).

⁸K. W. Schwarz, *J. Appl. Phys.* **85**, 108 (1999).

⁹M. Kammler, D. Chidambarro, K. W. Schwarz, C. T. Black, and F. M. Ross, *Appl. Phys. Lett.* **87**, 133116 (2005).

¹⁰S. Izumi, T. Miyake, S. Sakai, and H. Ohta, *Mater. Sci. Eng., B* **395**, 62 (2005).

¹¹K. Schwarz, *J. Appl. Phys.* **100**, 103507 (2006).

¹²V. V. Bulatov, S. Yip, and A. S. Argon, *Philos. Mag. A* **72**, 453 (1995).

¹³V. V. Bulatov, J. F. Justo, W. Cai, S. Yip, A. S. Argon, L. Lenosky, M. de Koning, and T. Diaz de la Rubia, *Philos. Mag. A* **81**, 1257 (2001).

¹⁴J. Godet, L. Pizzagalli, S. Brochard, and P. Beauchamp, *Phys. Rev. B* **70**, 054109 (2004).

¹⁵J. Godet, S. Brochard, L. Pizzagalli, P. Beauchamp, and J. M. Soler, *Phys. Rev. B* **73**, 092105 (2006).

¹⁶T. Zhu, J. Li, and S. Yip, *Phys. Rev. Lett.* **93**, 025503 (2004).

¹⁷J. Li, *MRS Bull.* **32**, 151 (2007).

¹⁸T. Zhu, J. Li, and S. Yip, *Phys. Rev. Lett.* **93**, 205504 (2004).

¹⁹F. H. Stillinger and T. A. Weber, *Phys. Rev. B* **31**, 5262 (1985).

²⁰J. Godet, L. Pizzagalli, S. Brochard, and P. Beauchamp, *Scr. Mater.* **47**, 481 (2002).

²¹J. A. Zimmerman, C. L. Kelchner, P. A. Klein, J. C. Hamilton, and S. M. Foiles, *Phys. Rev. Lett.* **87**, 165507 (2001).

²²W. C. Dash, in *Dislocations and Mechanical Properties of Crystals*, edited by J. C. Fisher, W. G. Johnston, R. Thomson, and T. Vreeland, Jr. (Wiley, New York, 1957), p. 57.

²³K. Wessel and H. Alexander, *Philos. Mag.* **35**, 1523 (1977).

²⁴J. Rabier and J. L. DemeNET, *Scr. Mater.* **45**, 1259 (2001).

²⁵A. Gomez, D. J. H. Cockayne, P. B. Hirsch, and V. Vitek, *Philos. Mag.* **31**, 105 (1975).

²⁶K. Sato, K. Hiraga, and K. Sumino, *Jpn. J. Appl. Phys., Part 2* **19**, L155 (1980).

²⁷Q. Ren, B. Joos, and M. S. Duesbery, *Phys. Rev. B* **52**, 13223 (1995).

²⁸M. S. Duesbery and B. Joos, *Philos. Mag. Lett.* **74**, 253 (1996).

²⁹J. R. Rice, *J. Mech. Phys. Solids* **40**, 239 (1992).

³⁰J. Godet, L. Pizzagalli, S. Brochard, and P. Beauchamp, *J. Phys.: Condens. Matter* **15**, 6943 (2003).

³¹Y. Juan and E. Kaxiras, *Philos. Mag. A* **74**, 1367 (1996).

³²T. Suzuki, T. Yasutomi, T. Tokuoka, and I. Yonenaga, *Philos. Mag. A* **79**, 2637 (1999).

³³J. Rabier and J. L. DemeNET, *Phys. Status Solidi B* **222**, 63 (2000).

³⁴J. Rabier and J. L. DemeNET, *Phys. Status Solidi A* **202**, 944 (2005).

³⁵Geometrical-nonlinear elastic calculation is done by using ANSYS 10.0. Periodic boundary conditions are applied. Elastic constants of the SW potential are used.

³⁶G. Henkelman and H. Jonsson, *J. Chem. Phys.* **113**, 9978 (2000).

³⁷G. Henkelman, B. P. Uberuaga, and H. Jonsson, *J. Chem. Phys.* **113**, 9901 (2000).

³⁸T. Zhu, J. Li, A. Samanta, H. G. Kim, and S. Suresh, *Proc. Natl. Acad. Sci. U.S.A.* **104**, 3031 (2007).

³⁹R. D. Boyer, Ph.D. thesis, MIT, 2007.

⁴⁰S. Izumi and S. Yip (unpublished).

⁴¹Y. Mishin, M. J. Mehl, D. A. Papaconstantopoulos, A. F. Voter, and J. D. Kress, *Phys. Rev. B* **63**, 224106 (2001).

⁴²L. Pizzagalli, P. Beauchamp, and J. Rabier, *Philos. Mag.* **83**, 1191 (2003).

⁴³J. R. Rice and R. Thomson, *Philos. Mag.* **29**, 73 (1974).

⁴⁴Y.-H. Chiao and D. R. Clarke, *Acta Metall.* **37**, 203 (1989).